African Journal of Biotechnology Vol. 12(10), pp. 1138-1147, 6 March, 2013
Available online at http://www.academicjournals.org/AJB
DOI: 10.5897/AJB12.1279
ISSN 1684–5315 ©2013 Academic Journals

Full Length Research Paper

Fingerprint motifs of phytases

Cheng-Ming Fan[1#], Ya-Hui Wang[2#], Chang-Ying Zheng[2] and Yong-Fu Fu[1*]

[1]MOA Key Lab of Soybean Biology (Beijing), National Key Facility of Crop Gene Resource and Genetic Improvement, Institute of Crop Sciences, Chinese Academy of Agricultural Sciences, 12 Zhongguancun Nandajie, Haidian District, Beijing 100081, China.
[2]College of Agronomy and Plant Protection, Qingdao Agricultural University, Qingdao, 266109, China.

Accepted 2 October, 2012

Phytate is the major form of phosphorus storage in plant seeds and the soil organic phosphorus. The phytase is a class of enzymes which catalyzes the hydrolysis of phytate and release free orthophosphoric acid. Motifs provide insight into protein structure, function and evolution. 39 fingerprint motifs were obtained in phytases through multiple EM for motif elicitation (MEME) analysis based on 54 whole phytase sequences with an average of 16.6% identity (ranging from 3.9 to 52.5%). The phytase family is classified into seven groups: HAPhys, PAPhys, BPPhys, BPRPhys, PTPhys, ALPhys and APPAs according to the phylogenetic analysis and motif characters. Every phytase group has its typical fingerprint motifs through motif alignment and search tool (MAST) results. Based on the phylogenetic tree and characteristics of phytase motif organisations, BPPhy family has 13 motifs, and is classified into five subgroups, BPPhy I to V. HAPhy with 11 motifs is classified into four subgroups, HAPhyI to IV. PAPhy, BPRPhy, PTPhy and APPAs have four, four, four and six fingerprint motifs, respectively, but no fingerprint motifs are found by MAST for ALPhys. In comparison with known crystal structures, motif fingerprints are relative to key amino acid residues of phytase activity, which make the features of different phytase groups known better based on their primary structures. Among the total of potential 173 phytases gained in 11 plant genomes through MAST, PAPhys are the major phytases, and HAPhys are the minor, and other phytase groups are not found *in planta*.

Key words: Phytase, fingerprint motif, multiple EM for motif elicitation (MEME), MAST.

INTRODUCTION

Phytate is the major form of phosphorus storage in plant seeds (Reddy et al., 1982; Raboy et al., 1984; Ma et al., 2012) and the soil organic phosphorus (Dalai, 1977; Selle et al., 2000). Although, phytate cannot be directly used by plants and monogastric animals, such as human, swine, poultry and fish, and therefore runs off into the soil or water leading to phosphorus environmental contamination (Mallin, 2000; Rao et al., 2009; Johnson et al., 2010).

Phytase is a class of phosphatases hydrolyzing phytate *in vitro* and releases at least one phosphate, lower inositol phosphates, and potentially chelated minerals (Chu et al., 2004). Therefore, phytase as a feed supplement improves the nutritional quality of phytate rich diets and eventually reduces environmental pollution.

*Corresponding author. E-mail: fuyf@caas.net.cn or fufu19cn@163.com.

[#]These authors contributed equally to this work.

Phytases are mainly found in plants, microorganisms as well as in some animals (Bitar and Reinhold, 1972;Cooper and Gowing, 1983; Wodzinski and Ullah, 1996; Dai et al., 2011; Jorquera et al., 2011).

Depending on the optimum pH for catalysis, phytases can be roughly classified into three groups: alkaline, acid or neutral ones. Alkaline phosphatase (ALP, PF00245 and EC 3.1.3.1) with phytase activity had been measured in the small intestine of rat, rabbit, guinea-pig and hamster (Cooper and Gowing, 1983; Zhang et al., 2011b; Yang et al., 2012).

Phytases from rat (*Rattus norvegicus*) shared very low sequence similarity with other known phytases, and their optimum pH for phytase activity was 7.5 (Yang et al., 1991). Alkaline phytases were also found in plant seeds (Scott, 1991; Dionisio et al., 2007) or pollens (Barrientos et al., 1994). The optimum pH for phytase activity of LlAlp1 and LlAlp2 with RHGXRXP and HD motifs from *Lilium longiflorum* is 7.3 and 8.3, respectively (Garchow et al., 2006), L lAlp1 and LlAlp2 share less similarity

with fungal histidine acid phytases than with mammalian multiple inositol polyphosphate phosphatases (MIPPs, EC 3.1.3.62) (Mehta et al., 2006), which are a distinct evolutionary group within the histidine phosphatase family (Chi et al., 1999).

Moreover, some phytases from *Bacillus* exhibit broad pH range of 5.0 to 8.0 (Haros et al., 2005; Chan et al., 2006; Gulati et al., 2007; Rao et al., 2008; Reddy et al., 2009; Zhang et al., 2011a). Acid phytases are also composed of many different protein families, such as histidine acid phosphatases (HAPs, EC 3.1.3.2) and purple acid phosphatises (PAPs, EC 3.1.3.2).

According to the initiation site of dephosphorylation of the phytate, there are three types of phytases: 3-phytases (EC 3.1.3.8), 4-phytases (or 6-phytases, EC 3.1.3.26) and 5-phytases (EC 3.1.3.72). On the basis of the catalytic mechanism or structural differences, phytases can be classed into three groups, such as HAPs, beta-propeller phytases (BPPs, EC 3.1.3.8) and PAPs (Tye et al., 2002; Mullaney and Ullah, 2003). HAPs with phytase activity share three motifs: the same active site sequence (RHGXRXP) (Ullah and Dischinger, 1993), conserved cysteine motifs directly associated with the formation of disulfide bridges, which confer their higher thermostability, and the catalytic dipeptide motif HD at C-terminal for substrate binding or product leaving (Kostrewa et al., 1997; Lee et al., 2003; Vohra and Satyanarayana, 2003; Mullaney and Ullah, 2005). BPPs have a six-bladed beta-propeller folding architecture (Ha et al., 2000) and dephosphorylate phytate in a stereospecific way by sequential removal of every second phosphate groups (Greiner et al., 2007).

BPPs exhibit both unique Ca^{2+}- dependent catalytic property and highly strict substrate specificity for the calcium-phytate complex (Fu et al., 2008). PAPs from different kingdoms share conserved phosphoesterase signature motifs, DXG, GDXXY, GNH[E/D], VXXH and GHXH, which cover seven key metal-ligating amino-acid residues (in bold) (Klabunde et al., 1996; Schenk et al., 2000; Olczak et al., 2003). Among them, animal PAPs contain a binuclear metallic center composed of two irons [Fe(III)-Fe(II)], whereas PAPs in plants, found as a homodimeric glycoprotein in most cases, one iron ion [Fe(III)] is joined by one zinc or manganese ion (Olczak et al., 2003; Dionisio et al., 2007).

PhyAsr, a phytase from the anaerobic ruminal bacterium *Selenomonas ruminantium* shares very low sequence homology with other microbial phytases, and has an active site: phosphate-binding loop (P-loop, H**C**XXGXXR) and WPD-loop forming the substrate binding pocket, which are features of protein tyrosine phosphatases (PTPs) (Chu et al., 2004; Puhl et al., 2007, 2008).

Phytases are very important to reuse environmental organic phosphorus and to decrease phosphorus pollution, and phytase is a superfamily containing members of several protein families, such as phytase (PF02333), HAP (PF00328), PAP and PTP. Every family should have its fingerprint motifs, and motifs provide insight into protein structure, function and evolution.

Although, up to now, the fingerprint motifs of phytases has not been systematically reported according to our knowledge. In this study, the fingerprint motifs and relationships between motifs and key active amino acid residues were investigated among HAPhys, PAPhys, BPPhys, BPRPhys, PTPhys, ALPhys and APPAs. So, multiple EM for motif elicitation (MEME) software was employed to investigate the motif fingerprints of different phytases. According to MEME results, motif alignment and search tool (MAST) software was further applied to analyze the fingerprint motifs of phytases and types of phytases in 11 plant genomes.

METHODS

Phytase sequences retrieval

Phytase was used as a key word to search the Protein Knowledgebase (UniProtKB) (http://www.uniprot.org/uniprot) to find existing phytase sequences (additional file 1). Only whole length sequences were selected, but if a species has only a known partial sequenced phytase, it would be selected.

Identifying model phytase sequences

One model sequence represented one species to ensure the species diversity. And when one species had more than one phytase sequences, multiple sequence alignments in ClustalX1.8 were used to filter highly identical (identity more than 80%) sequences in one species (Thompson et al., 1994), but for plants, all the known phytase were selected, because the known plant phytases are very few.

Motif identification

The conserved motifs of model phytases were dug out through analysis by MEME version 4.4.0 (http://meme.sdsc.edu/meme/intro.html) (Bailey et al., 2010). To reduce the bias on the conserved motif search, highly similar above model sequences were removed using PURGE to get MEME model sequences to identify the fingerprint motifs of different phytase families (Neuwald et al., 1995). Maximum number of motifs found was 50, and the minimum motif length was six amino acids (AAs), other arguments were default and then, motifs were analyzed through the web site (http://motif.genome.jp/) and the critical active sites of BPPhys, HAPhys, PTPhys, PAPhys and APPAs were identified based on sequence comparison and structural analysis of phytases from *Bacillus amyloliquefaciens* (Shin et al., 2001), *Aspergillus fumigatus* (Xiang et al., 2004), *S. ruminantium* (Chu et al., 2004), *Phaseolus vulgaris* (Strater et al., 1995) and *Escherichia coli* (Lim et al., 2000), respectively to investigate the relationship between the formation of active sites and motifs.

Phylogenetic reconstruction

Phylogenetic and molecular evolutionary analyses were done using MEGA version 4.0.2 through the neighbor-joining algorithm (Tamura et al., 2007).

Analyzing motif profiles in different phytase families and investigating plant phytases in the genome level

According to the MEME motif results, MAST (http://meme.sdsc.edu/meme4_5_0/cgi-bin/mast.cgi) was applied to analyze the motif profiles of 233 different phytases and to search potential phytases in plant genomes (Bailey and Gribskov, 1998). The E-value was less than 1e-10 and other parameters were default.

Eleven (11) plant genomes sequences, including *Arabidopsis thaliana* (At), *Brachypodium distachyon* (Bd), *Glycine max* (L.) Merr. (Gm), *Medicago truncatula* (Mt), *Oryza sativa* ssp. *japonica* (Os), *Physcomitrella patens* subsp. *patens* (Pp), *Populus trichocarpa* (Pt), *Selaginella moellendorffii* (Sm), *Sorghum bicolour* (Sb), *Vitis vinifera* (Vv) and *Zea mays* (Zm) had been downloaded through Superfamily (http://supfam.mrc-lmb.cam.ac.uk/SUPERFAMILY/cgi-bin/taxonomic_gen_list.cgi).

RESULTS

Identification of model phytases

A total of 984 peptide sequences with annotation of 'phytase' were found in databanks UniProt Proteins, and based on the annotations, histidine acid phosphatases, purple acid phosphatases, beta-propeller phytases, protein tyrosine phosphatases and alkaline phosphatases, phosphatases with EFG-like domain, and acid phosphatase/phytase A had potential phytase functions. To show their special phytase characteristics, they were short for HAPhy, PAPhy, BPPhy, PTPhy, ALPhy, EGF-Phy and APPA in this study, respectively.

There are 329 out of the 984 sequences that are the whole coding sequences, and then, highly similar sequences in the same species were filtered through multiple sequence alignment by clustalw1.8. Finally, 233 unique sequences including 131 prokaryotic and 102 eukaryotic phytase sequences covered phytases from 190 species including 131 bacterium sequences, 70 fungus sequences, 27 plant sequences, one animal sequence and four yeast sequences.

For motif analysis, 54 sequences were randomly screened out as MEME model sequences from 233 sequences through PURGE analysis, of which no two sequences had a local alignment score greater than 250. Their average similarity was 16.6% (ranging from 3.9 to 52.5%).

To identify different phytase families, every model sequence must have at least one or more motifs. For that, maximum number of motifs to be found by MEME was set from 10 to 50. There were 44 different motifs in total found among 54 MEME model sequences (Table 1). The relationships between the motifs and active sites are shown as follows.

BPPhy family

According to MAST results, fingerprint motif 2, 7 (or 40 and 22), 9, 23, 16, 1, 15, 10, 3, 4 (or 11) and 6 occur from N to C terminals of BPPhys. Motif 1, 2, 3, 9 and 10 were conserved in all the BPPhys, while motif 4 and 11 did not occur together, as well as motif 7 or 40 and 22, and main BPPhy motif organisations were five architectures. For example, BPPhy I was composed of motif 2, 7, 9, 16, [23], 1, [15], 10, 3, 4/11 and 6; BPPhy II, motif 26, 19, 37, 17, 2, 40, 22, 9, 1, 10, 3, 4 and 6; BPPhy III, motif 2, 40, 22, 9, 33, [15], 10, 3, 4/11 and [6]; BPPhy IV (EGF-Phy), motif [9], [10], [41], 2, 7, 9, 23, 1, 15, 10, 3, 4 and [6]; BPPhy IV, motif 2, 40, 22, 9, 23, 1, 15, 10, 3, 4 and [6] (note: '[ ]' showed the motif can be found or not, and '/' showed one of the two motifs can be found). C terminals of BPPhys were relatively conserved, but the motifs in the N terminals were diversity (additional file 2).

Based on an known crystal structure of phytase (O66037) from *B. amyloliquefaciens* (Ha et al., 1999; Shin et al., 2001), there are seven Ca^{2+} binding sites found, such as Ca1 (Glu43, Asp308, Asn339, Ile340 and Asp341), Ca2 (Asp308, Gly309, Asn336 and Glu338), Ca3 (Asp56, Pro57 and Val101), Ca4 (Asp55 and Glu211), Ca5 (Tyr159, Glu211, Glu227 and Glu260), Ca6 (Asp258, Glu260 and Gln279) and Ca7 (Asp52 and Asp314) (Shin et al., 2001). Therefore, the most binding site residues belonged to motif 2 (51 to 77), 7 (82 to 102), 16 (151 to 164), 1 (208 to 230), 10 (255 to 265), 3 (269 to 289 and 4 (307 to 337), respectively, except Ca1 (Glu43, Asn339, Ile340 and Asp341) and Ca2 (Glu338) which was not covered up. However, Asn339, Ile340, Asp341 and Glu338 were in fragment between motif 4 and 6 (348 to 362).

BPPhys exhibit unique Ca^{2+}-dependent catalytic property and contain six calcium binding sites. Three high-affinity binding sites (Ca1, Ca2 and Ca3) are responsible for thermostability, whereas three low-affinity binding sites (Ca4, Ca5 and Ca6) are responsible for catalytic activity (Ha et al., 2000). Additionally, BPPhys have two phosphate binding sites: the "cleavage site", which is responsible for the hydrolysis of a substrate, and the "affinity site", which increases the binding affinity for substrates containing adjacent phosphate groups, and the seventh calcium binding site is only present in the presence of phosphate ions (Shin et al., 2001).

According to phytase motif fingerprints, EGF-Phys from fungus did not show obvious difference with BPPhys except an EGF-like domain (motif 41). In this case, they were classified into BPPhy group in this study.

HAPhy family

HAPhy family is the first known phytase family and now composed of many members. According to the MAST results, its conserved motifs were motif 5, 18, 14, 8 and 30, and motif 5 and 27 or 13 contained motif RHGXRXP and HD (additional file 3), respectively. Main HAPhy motif organisations were four sub-groups, that is, HAPhyI was comprised of motif 39, 5, 28, 18, 14, 8, 27, 30 and 20; HAPhyII, motif 5, 28, 18, 14, 8, 27, and 30; HAPhyIII,

Table 1. Main fingerprint motifs of every phytase family.

Motif	Width	Best possible match sequence
BPPhys		
1	23aa	SQIEGCVVDEETGQLYIGEEDVG
2	27aa	GDDADDPAIWVHPTDPEKSLIIGTDKK
3	21aa	NGQGYLIVSSQGNNSYAVYRR
4	31aa	IDGVSETDGIEVTNVPLGEHFPHGLFVVQDG
6	15aa	QNFKYVDWRDIAKAF
7	21aa	VYDLDGKQVQYLPVGRMNNVD
9	20aa	VDIAVASNRSHNKLCVFKID
10	11aa	LVADVEGLTIY
11	29aa	DGVSHTDGIDVHSYALPGFPEGMLVVQDG
15	9aa	IWKYPAEPE
16	14aa	IPTDMNEPYGMCLY
22	15aa	PKRYNNVDLEYGFML
23	20aa	TGKIYVFVNRKNGRIEQYEW
40	15aa	GLYVYDLQGRMIQHI
41	15aa	CYACLQNARCCCWRC
HAPhys		
5	21aa	IPEGCELEHVHILSRHGVRYP
8	50aa	SPFCDLFTQEEWHSYEYYQDLQWYYCYGPGNPLMAAQGVGYVNELLSRLT
13	25aa	KWTFLVGHDTNIAYIRTMLGFKWQL
14	21aa	PGMNLTAMDVSHMMDMCPYET
18	21aa	VRASSQQRVRKSAQWFLKGFF
20	37aa	YVRILVNDRVVPLHGCESDPGYRCKLEDYVEIMNYAR
27	29aa	HFPLHRALYADFSHDNQMVAIFSAMGLYN
28	29aa	WEYMLGHDHLTPFGEQQMINMGVSIYQRY
30	20aa	YVHSWIVPFAARMYIEKMSC
35	30aa	HMICKFYQYVRENHADGFKQRWSDWLAAHQ
38	26aa	YRQHCKIAMNYPDHISFWWNYMNTTE
39	11aa	HYWGQYSPFFS
APPAs		
5	21aa	IPEGCELEHVHILSRHGVRYP
13	25aa	KWTFLVGHDTNIAYIRTMLGFKWQL
18	21aa	VRASSQQRVRKSAQWFLKGFF
24	40aa	QPMDQVAWGKITSEQQWSQLLSLHNAQYDLMNKMPYIAQH
25	23aa	MQQVTPRKWPKWPVPYGWLTPRG
31	17aa	QCDNIPPGGKLVFERWQ
PAPhys		
21	50aa	WLIVGWHAPWYNSNKAHYMEGECMRVAMEKWFYKYKIDIVFTGHVHAYER
29	41aa	CWDRQPDYSAFREASFGHGILQVKNETHAVWKWHRNDDGKH
34	29aa	RWDYWGRFMERVTAYQPWMWNEGNHEIEQ
36	24aa	YKSGIIHHCRVDGLEYGTKYYYKC
BPRPhys		
7	21aa	VYDLDGKQVQYLPVGRMNNVD
10	11aa	LVADVEGLTIY
17	27aa	DNIEGMTWGPRLPDGRRSIVLVSDDNF
19	34aa	SGIRNNKGFEGMTISPDGSTLYAAMENPLVQDGP
26	27aa	DPAHGEYYAISDDRSEHGPVRFYTLDI
37	36aa	SFLVMERSYIPGQGNTKKIYEVDLRGATDVLDVEWL
PTPhys		
12	29aa	MPKHAWLHFHCQAGQGRTTTFMIMYDIMK

Table 1. Continued.

32	43aa	PIWIIDLRQESHGFFNEDPVSWHGVKNWANLGMSKAEVIKDER
35	30aa	HMICKFYQYVRENHADGFKQRWSDWLAAHQ
42	28aa	KNGMHYVRIPATDHKWPSYQMIDDFVNF

motif 5, 18, 14, 8, 27/13, 30, 20, and 38; HAPhyIV, motif 5, 28, 18, 35, 14, 8 and 30, and the members of HAPhyIV were all from plants, such as phytases from wheat (TaPhyIIc, A0FHB3), barley (HvPhyIIa1, A0FHA7) (Dionisio et al., 2007) and two from *Lilium longiflorum* [LlAlp1, (Q0GYS1) and LlAlp1 (Q0GYS2)] (Mehta et al., 2006).

Aspergillus fumigatus phytase (O00092) (Xiang et al., 2004) is a typical HAPhys. The conserved catalytic residues of *A. fumigatus* phytase are composed of a catalytic motif of R80H81GXRXP86 and a substrate binding motif of H359D360, which were embraced by motif 5 (66 to 86) and 27 (348 to 376), respectively. The catalytic residue His81 is at the center and closely surrounded by four positively charged residues (Arg80, Arg84, Arg164 and His359) and one negatively charged residue (Asp360). These residues are embedded in motif 5 (66 to 86), 18 (157 to 177) and 27 (346 to 374). Besides the key residues above, *A. fumigatus* phytase has five disulfide bonds presented at positions 30-39, 70-412, 213-463, 262-280 and 434-442, which are important to phytase catalytic properties, especially at optimum temperature and pH (Mullaney et al., 2010). Motif 5, 14 (246 to 266), 8 (277 to 326), 30 (395 to 414) and 20 (419 to 455) contained Cys70, 262, 280, 434, and 442, and only two potential N-linked glycosylation sites (Asn350 and Asn374) can be also found in the motifs above, and another four (Asn104, Asn205, Asn228, and Asn337) were beyond this motif.

Another phytase crystal structure from *Aspergillus niger* (P34752) (Oakley, 2010) was selected to analyze the relationship between active residues and their motifs. Motif 5 (67 to 87) and 27 (348 to 376) contained motif RHGXRXP and HD motif, respectively. Motif 5, 14 (246 to 266), 8 (277 to 326) and 20 (419 to 455) contained Cys71, Cys264, Cys282, Cys436 and Cys444, which can form disulfide bonds, even though these motifs do not include other disulfide-bond residues (Cys31-Cys40 and Cys215-Cys414). Similarly, only two potential N-linked glycosylation sites (Asn339 and Asn352) were embraced in motif 27, and others (Asn27, Asn59, Asn105, Asn120, Asn207, Asn230, Asn376 and Asn388) were absent in all motifs.

APPA family

According to the crystal structure of a phytase from *E. coli* (P07102), the crucial residues involved in phytate binding are Arg38, Thr45, Lys46, Asp110, Arg114, Ser234, Ser237, Met238, Arg289, His325, Asp326 and Thr327 (Lim et al., 2000). Motif 5 (23 to 45), 18 (107 to 127), 24 (250 to 289) and 13 (318 to 342) contained eight key residues except Lys46, Ser234, Ser237 and Met238. Motif 5, 18, 44 (130 to 158), 24, 13 and 31 (345 to 361) contained the key residues binding Hg^{2+}, such as Hg1 (His135 and Thr349), Hg3 (Arg38, His272, Asp347 and Asp326), and Hg4 (His272, Asp347, and Thr349) except Hg2 (His304, Gln309 and Leu315). So fingerprint motifs of APPA were motif 5, 18, 44, 24, 13 and 31 (additional file 4) (Table 2).

PAPhy family

The fingerprint motifs were motif 36, 34, 21 and 29 for this family. Motif 36 was similar to partial sequences of PhoD-like phosphatases (PF09423), while motif 34 and 21 were similar to partial sequences of calcineurin-like phosphoesterases (PF00149). Three conversed motifs of PAPhys, GNHED, VXXH and GH[V/D] (Klabunde et al., 1996; Schenk et al., 2000; Olczak et al., 2003) were included in motif 34 and 21, while another two motifs, DXG and GDXXY, were sited between motif 36 and 34.

All members of this group contain a characteristic set of seven amino-acid residues involved in metal-ligation, which included five conserved motifs (Olczak et al., 2003). Animal PAPhys contain a binuclear metallic centre composed of two irons, whereas in plants PAPhys, one iron ion is joined by one zinc or manganese ion (Klabunde et al., 1995; Battistuzzi et al., 1997; Schenk et al., 1999; Olczak et al., 2003). But Ca^{2+} and Zn^{2+} stimulate the phytase activity of AtPAP15 (127.5 and 129.4%, respectively), while Mn^{2+} exhibits no effects on phytase activity (Kuang et al., 2009). So, motif 36, 34, and 21 were very important for PAPhy function (additional file 5).

PTPhy family

In PTPhy family, motif 32, 42, 12 and 35 stood for the motif profiles of PTPhys in that order (additional file 6). In PhyAsr, *S. ruminantium* phytase (Chu et al., 2004), the binding phytate loop, WPD-loop (223-227), and the active site phosphate-binding loop, P-loop (251–258) (Chu et al., 2004; Gruninger et al., 2008), were included in motif 42 (211-238) and motif 12 (242-270), respectively. Asp223 in the motif 42 is unique because it is phytase active

(Puhl et al., 2007).

BPRPhy family

B1WU04, D4TEW0, C8RSN7, D5PPT3, A0QQJ0 and A4FR55 contained motif 26, 19, 37 and 17 (additional file 7), and motif 19 was similar to partial sequence of a beta-propeller repeats protein family from unknown function protein family (PF05787). However, four motifs were similar to the N-terminal of some BPPhy members, which is not the known phytase domain. So their phytase characteristics should be confirmed in the future.

ALPhys motifs

Among 54 MEME model phytase sequences, rat intestinal-type alkaline phytase (P51740) (Yang et al., 1991), fungus alkaline phosphatase (C8VPB9 from *A. nidulans*) and maize PhyT II (Q9ZRQ5) (Maugenest et al., 1999) were selected as the model ALPhys, but P517406, C5G6T3, C8VPB9, B6QCU5, A1CL92, A1D620 and Q4WYS0, which were annotated as ALPs, did not share any of the 44 motifs based on the MAST results. While three maize phytases, PhyS11 (P93644) (Maugenest et al., 1997), PhyTI (Q9T0N7) and PhyTII (Q9ZRQ5) (Maugenest et al., 1999) had motif 41, 32, 20 and 2.

Phylogenetic analysis

A total of 233 phytase sequences above including 131 prokaryotic and 102 eukaryotic phytases were selected to reconstruct a phylogenetic tree through MEGA 4.0.2. As shown in Figure 1, 233 phytases can be classified into seven groups on the topological tree: HAPhy, PAPhy, BPPhy, PTPhy, BPRPhy, ALPhy and APPA. Eukaryotic phytases can be classified into four groups, such as HAPhy, PAPhy, EGF-Phy and ALPhy, while prokaryotic phytase family can be classified into another four groups, such as BPPhy, APPA, PTPhy and BPRPhy, suggesting that there was much difference of phytases between eukaryotic and prokaryotic family.

Based on motif organisations, EGF-Phys were not obviously different with BPPhys in the phytase domain, so EGF-Phys should belong to a sub-group of BPPhys.

Phytases in some completely sequenced plant genomes

Phytases are very important to improve plant abilities to use organic phosphate, as well as to increase crop production. To get the potent plant phytases and analyze their characteristics, 11 model plants were included in the survey of phytases. According to the MAST results, 160 PAPhys were found in plants, 13 HAPhys were found, but no other kind of phytases was found (additional file 8).

DISCUSSION

A motif is a sequence pattern that occurs repeatedly in a group of related biological sequences. MEME is one of the most widely used tools for searching motifs in sets of biological sequences (Bailey et al., 2006, 2010). And MAST is another tool for searching biological sequence databases for sequences that contain one or more of a group of known motifs (Bailey and Gribskov, 1998). So, the architectures of similar biological sequences can be known through the combined analysis of MEME and MAST (Bailey and Gribskov, 1998; Bailey et al., 2010), and they can detect significant pairwise similarity between any of the sequences and the repeats present in the phytases, and partially analyze the characters of phytase primary structures.

Phytases are classified into various groups with different criteria by different researchers. Therefore, different groups share same phytases, and it is difficult to distinguish among them. In addition, classification known does not reflect the enzymatic mechanism of catalysis on phytate. Phytases are variable in sequences and structures, but their catalysis on phytate is relatively steady. The catalysis is determined by the conserved enzyme active sites, substrates or ion binding sites and other key sites, and these key sites form the fingerprint motifs. Motifs can make it clear to distinguish organisation characters of different phytase groups. Our results show that different family had their distinct motifs and their special organization, and most of crucial active residues were embraced in these motifs. Also, the results indicate that eukaryotic and prokaryotic phytases had distinct motif structure, which may confer subfunctionalization during the evolutional progress of phytases.

BPPhy was the major phytase family in prokaryotes, even though the peptides' length of BPPhys was variable from 331 to 2698 aa, the phytase domain was highly conserved among them. The segment from motif 2 to 6 in every group was the important phytase domains based on Pfam knowledge. Five sub-groups were sub-classified mainly according to the phytase domains (the segment from motif 2 to 6), and more subgroups would occur based on motif organisations, for example, some (Q9A8Q8 and D5VH79) had double whole phytase domains. Besides phytase motifs, some non-phytases motifs were also found. For example, BPPhys (BPPhy II) from cyanobacterium contained PhoD domain, as well as fungus BPPhys (BPPhy IV) containing EGF-like domain, and their function in phytase activity should be tested in the future.

HAPhy was the major phytase family in animals and yeast, and were identified much earlier than other families. There were subgroups in this family, but any special motif organisations for each subgroups were not found, so they were classified as a whole family. For example, two alkaline phytases from lily pollen, LlAlp1

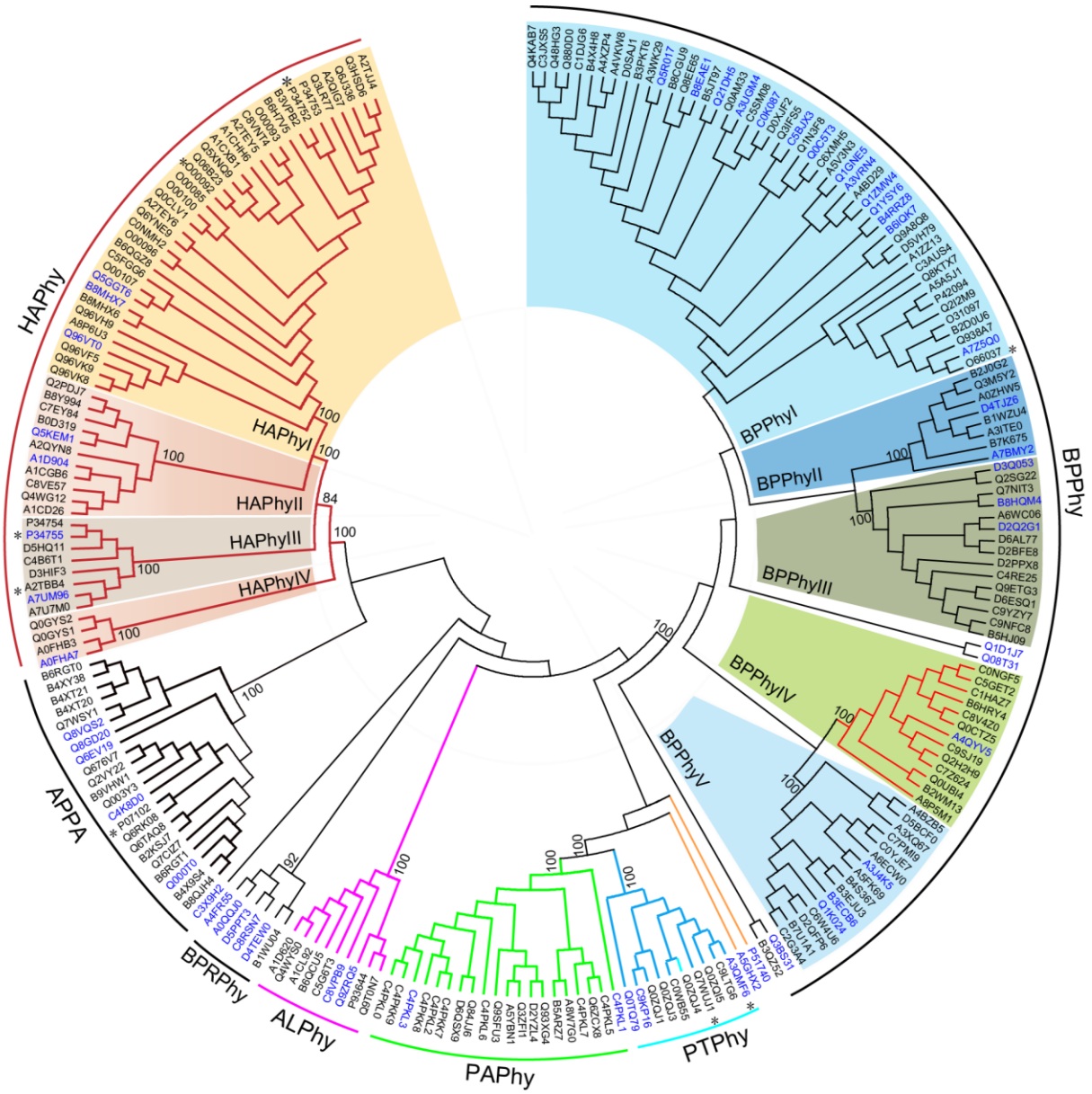

Figure 1. Phytases from plants, microorganism and animals. Phytases were selected to analyze the fingerprint motifs in the blue colour. Additional file 1 is for 233 phytases information. Crystal structures of phytases are marked by asterisk. Phytases are from eukaryotes with colour branches and from prokaryotes with black branches. BPPhy family was classified into 5 subgroups, BPPhyI, BPPhyII, BPPhyIII, BPPhyIV and BPPhyIV with different colour background. HAPhy family is classified into 4 subgroups, HAPhyI, HAPhyII, HAPhyIII and HAPhyIV with different colour background.

(Q0GYS1) and LlAlp2 (Q0GYS2), shared <25% similarity in sequence with fungal histidine acid phytases and most closely related to MIPPs from humans (25%) and rats (23%) (Mehta et al., 2006). Other four MIPPs from wheat seeds, TaPhyIIa1 (A0FHB0), TaPhyIIa2 (A0FHB1), TaPhyIIb (A0FHB2), and TaPhyIIc (A0FHB3), and three MIPPs from barley seeds, HvPhyIIa1(A0FHA7), HvPhyIIa2 (A0FHA8) and HvPhyIIb(A0FHA9), showed the activity of acid phytase with narrow substrate specificity (Dionisio et al., 2007), but they shared similar motifs with other HAPhys and formed a subgroup of HAPhys. In HAPhy family, the pH affects the substrate specificity, and acid phytases have narrow substrate specificity, unlike alkaline phytases (Wyss et al., 1999).

Motifs 5 and 18 were found in two phytase groups, HAPhys and APPAs. Motif 5 contained the active motif RHGXRXP. The catalytic residue His of RHGXRXP motif is very important for HAPhys by forming phytate binding-site spatial structure (Xiang et al., 2004), but in the motif of APPAs, His mutating to Ala is unlikely to affect phytate

binding (Lim et al., 2000). HD motif, was another key motif of HAPhys (included in motif 27), and also APPAs (included in motif 13), but except His and Asp, other residues in motif 27 and 13 were different. The conserved amino acid-residue next to HD of motif 27 was Asn, while in motif 13 it was Thr. Thr was one key residue for phytate binding site (Lim and Jia, 2002), and there was no Thr in HAPhys. In this case, phytases with RHGXRXP motif and HD motif could be classified into two groups, HAPhys and APPAs.

There was no special motif found in ALPhys. Neither a rat (*Rattus norvegicus*) alkaline phytase (P51740) (Yang et al., 1991) nor a fungus alkaline phytase (A5GHX2) was clustered into ALPhys group according to the phylogenetic tree (Figure 1), and except three maize phytases (P93644, Q9T0N7 and Q9ZRQ5), other members of ALPhys did not share same motifs. For these three maize phytases, they were classed into HAPhys in the previous research (Maugenest et al., 1997, 1999). However, they lacked the rigorous phosphate-binding motifs RHGXRXP and HD, the characteristic motifs of HAPhys (Wodzinski and Ullah, 1996), suggesting some unknown motifs present in HAPhys for phosphate-binding. But HAPhys shared only 15.5% sequence similarity to PhyA (O00092), belonging to HAPhys. So ALPhys may be a large protein family and contain different groups, or the relationship among known ALPhys was too low to form its special motifs.

It is well known that phosphorus is an essential mineral for all living organisms, but available phosphorus for plant is very low in the soil, and organic phosphorus such as phytate is so much as to result in the phosphorus environmental contamination (Mallin, 2000; Rao et al., 2009; Johnson et al., 2010). So, improving the plant absorbing phosphorus is very important to increase the crop production and decrease the environmental contamination. Heterogenous expression of phytase in plants (Zhang et al., 2010b), a new phytase exploration (Zhang et al., 2010a), and analysis of phytase activities (Mullaney et al., 2010; Shivange et al., 2010; Zhao et al., 2010; Zhu et al., 2010) are focused on by many researchers. Our results show that the families of phytases in plants were quite different from that in other organisms, suggesting plants phytases had distinct mechanism for phytate utilization of phytases from animals and microbes. Only two phytase groups, PAPhy and HAPhy, were found in plants, and HAPhys are very few in plants. Up to date, the plant phytases mostly belong to PAPhys, only four plant phytases belong to HAPhys.

ACKNOWLEDGEMENTS

This work was partly supported by Transgenic Program (2009ZX08009-133B), the Chinese National Key Basic Research ‘‘973’’ Program (2010CB125906) and the National Natural Science Founds (31000680).

Research ‘‘973’’ Program (2010CB125906) and the National Natural Science Founds (31000680).

Additional files

Additional file 1, Fingerprint motif organisations and sequence information. The numbers in Motif organisations shown different motifs of phytases through MAST analysis. Motifs with color background are in the conserved sections of the protein families.
Additional file 2 Fingerprint motif logos of BPPhys. The logos of the conserved motifs were gained by MEME 4.0 (http://meme.nbcr.net/meme/).
Additional file 3 Fingerprint motif logos of HAPhys. The logos of the conserved motifs were gained by MEME 4.0 (http://meme.nbcr.net/meme/).
Additional file 4 Fingerprint motif logos of APPAs. The logos of the conserved motifs were gained by MEME 4.0 (http://meme.nbcr.net/meme/).
Additional file 5 Fingerprint motif logos of PAPhys. The logos of the conserved motifs were gained by MEME 4.0 (http://meme.nbcr.net/meme/).
Additional file 6 Fingerprint motif logos of PTPhys. The logos of the conserved motifs were gained by MEME 4.0 (http://meme.nbcr.net/meme/).
Additional file 7 Fingerprint motif logos of BPRPhys. The logos of the conserved motifs were gained by MEME 4.0 (http://meme.nbcr.net/meme/).
Additional file 8 Phytases in 11 completely sequenced plant genomes. All the genome database were downloaded from phytozome 8.0 (http://www.phytozome.net).And the phytase-like proteins from each plant were classified according the finger motifs.

REFERENCES

Bailey T, Boden M, Whitington T, Machanick P (2010). The value of position-specific priors in motif discovery using MEME. BMC Bioinform. 11:179.

Bailey TL, Gribskov M (1998). Combining evidence using p-values: application to sequence homology searches. Bioinformation 14:48-54.

Bailey TL, Williams N, Misleh C, Li WW (2006). MEME: discovering and analyzing DNA and protein sequence motifs. Nucleic Acids Res. 34:W369-373.

Barrientos L, Scott JJ, Murthy PP (1994). Specificity of hydrolysis of phytic acid by alkaline phytase from lily pollen. Plant Physiol. 106:1489-1495.

Battistuzzi G, Dietrich M, Locke R, Witzel H (1997). Evidence for a conserved binding motif of the dinuclear metal site in mammalian and plant purple acid phosphatases: 1H NMR studies of the di-iron derivative of the Fe(III)Zn(II) enzyme from kidney bean. Biochem. J. 323(Pt 3):593-596.

Bitar K, Reinhold JG (1972). Phytase and alkaline phosphatase activities in intestinal mucosae of rat, chicken, calf, and man. Biochim. Biophys. Acta. 268:442-452.

Chan WL, Lung SC, Lim BL (2006). Properties of beta-propeller phytase expressed in transgenic tobacco. Protein Exp. Purif. 46:100-106.

Chi H, Tiller GE, Dasouki MJ, Romano PR, Wang J, O'Keefe RJ, Puzas JE, Rosier RN, Reynolds PR (1999). Multiple inositol polyphosphate

phosphatase: evolution as a distinct group within the histidine phosphatase family and chromosomal localization of the human and mouse genes to chromosomes 10q23 and 19. Genomics 56:324-336.
Chu HM, Guo RT, Lin TW, Chou CC, Shr HL, Lai HL, Tang TY, Cheng KJ, Selinger BL, Wang AH (2004). Structures of Selenomonas ruminantium phytase in complex with persulfated phytate: DSP phytase fold and mechanism for sequential substrate hydrolysis. Structure 12:2015-2024.
Cooper JR, Gowing HS (1983). Mammalian small intestinal phytase (EC 3.1.3.8). Br. J. Nutr. 50:673-678.
Dai F, Qiu L, Ye L, Wu D, Zhou M, Zhang G (2011). Identification of a phytase gene in barley (*Hordeum vulgare* L.). PLoS One 6:e18829.
Dalai RC (1977). Soil Organic Phosphorus. In Advances in Agronomy. N.C. Brady, ed (Academic Press). pp. 83-117.
Dionisio G, Holm PB, Brinch-Pedersen H (2007). Wheat (*Triticum aestivum* L.) and barley (*Hordeum vulgare* L.) multiple inositol polyphosphate phosphatases (MINPPs) are phytases expressed during grain filling and germination. Plant Biotechnol. J. 5:325-338.
Fu S, Sun J, Qian L (2008). Effect of Ca^{2+} on beta-propeller phytases. Protein Pept. Lett. 15:39-42.
Garchow BG, Jog SP, Mehta BD, Monosso JM, Murthy PP (2006). Alkaline phytase from *Lilium longiflorum*: purification and structural characterization. Protein Exp. Purif. 46:221-232.
Greiner R, Lim BL, Cheng C, Carlsson NG (2007). Pathway of phytate dephosphorylation by beta-propeller phytases of different origins. Can. J. Microbiol. 53:488-495.
Gruninger RJ, Selinger LB, Mosimann SC (2008). Effect of ionic strength and oxidation on the P-loop conformation of the protein tyrosine phosphatase-like phytase. PhyAsr. FEBS J. 275:3783-3792.
Gulati HK, Chadha BS, Saini HS (2007). Production and characterization of thermostable alkaline phytase from *Bacillus laevolacticus* isolated from rhizosphere soil. J. Ind. Microbiol. Biotechnol. 34:91-98.
Ha NC, Kim YO, Oh TK, Oh BH (1999). Preliminary X-ray crystallographic analysis of a novel phytase from a *Bacillus amyloliquefaciens* strain. Acta Crystallogr. D. Biol. Crystallogr. 55:691-693.
Ha NC, Oh BC, Shin S, Kim HJ, Oh TK, Kim YO, Choi KY, Oh BH (2000). Crystal structures of a novel, thermostable phytase in partially and fully calcium-loaded states. Nat. Struct. Biol. 7:147-153.
Haros M, Bielecka M, Sanz Y (2005). Phytase activity as a novel metabolic feature in Bifidobacterium. FEMS Microbiol. Lett. 247:231-239.
Johnson SC, Yang M, Murthy PP (2010). Heterologous expression and functional characterization of a plant alkaline phytase in *Pichia pastoris*. Protein. Expr. Purif. 71(2):196-203.
Jorquera MA, Crowley DE, Marschner P, Greiner R, Fernandez MT, Romero D, Menezes-Blackburn D, De La Luz Mora, M (2011). Identification of beta-propeller phytase-encoding genes in culturable *Paenibacillus* and *Bacillus* spp. from the rhizosphere of pasture plants on volcanic soils. FEMS Microbiol. Ecol. 75:163-172.
Klabunde T, Strater N, Frohlich R, Witzel H, Krebs B (1996). Mechanism of Fe(III)-Zn(II) purple acid phosphatase based on crystal structures. J. Mol. Biol. 259:737-748.
Klabunde T, Strater N, Krebs B, Witzel H (1995). Structural relationship between the mammalian Fe(III)-Fe(II) and the Fe(III)-Zn(II) plant purple acid phosphatases. FEBS Lett. 367:56-60.
Kostrewa D, Gruninger-Leitch F, D'Arcy A, Broger C, Mitchell D, van Loon AP (1997). Crystal structure of phytase from *Aspergillus ficuum* at 2.5 A resolution. Nat. Struct. Biol. 4:185-190.
Kuang R, Chan KH, Yeung E, Lim BL (2009). Molecular and Biochemical Characterization of AtPAP15, a Purple Acid Phosphatase with Phytase Activity, in *Arabidopsis*. Plant Physiol. 151(1):199-209.
Lee DC, Cottrill MA, Forsberg CW, Jia Z (2003). Functional insights revealed by the crystal structures of *Escherichia coli* glucose-1-phosphatase. J. Biol. Chem. 278:31412-31418.
Lim D, Jia Z (2002). Heavy metal-mediated crystallization of *Escherichia coli* phytase and analysis of bridging interactions. Protein Pept. Lett. 9:359-365.
Lim D, Golovan S, Forsberg CW, Jia Z (2000). Crystal structures of *Escherichia coli* phytase and its complex with phytate. Nat. Struct. Biol. 7:108-113.
Ma XF, Tudor S, Butler T, Ge Y, Xi Y, Bouton J, Harrison M, Wang ZY (2012). Transgenic expression of phytase and acid phosphatase genes in alfalfa (*Medicago sativa*) leads to improved phosphate uptake in natural soils. Mol. Breed. 30:377-391.
Mallin MA (2000). Impacts of industrial animal production on rivers and estuaries. Am. Sci. 88(1):26-27.
Maugenest S, Martinez I, Godin B, Perez P, Lescure AM (1999). Structure of two maize phytase genes and their spatio-temporal expression during seedling development. Plant Mol. Biol. 39:503-514.
Maugenest S, Martinez I, Lescure AM (1997). Cloning and characterization of a cDNA encoding a maize seedling phytase. Biochem. J. 322(Pt 2):511-517.
Mehta BD, Jog SP, Johnson SC, Murthy PP (2006). Lily pollen alkaline phytase is a histidine phosphatase similar to mammalian multiple inositol polyphosphate phosphatase (MINPP). Phytochemistry 67:1874-1886.
Mullaney EJ, Locovare H, Sethumadhavan K, Boone S, Lei XG, Ullah AH (2010). Site-directed mutagenesis of disulfide bridges in *Aspergillus niger* NRRL 3135 phytase (PhyA), their expression in *Pichia pastoris* and catalytic characterization. Appl. Microbiol. Biotechnol. 87:1367-1372.
Mullaney EJ, Ullah AH (2003). The term phytase comprises several different classes of enzymes. Biochem. Biophys. Res. Commun. 312:179-184.
Mullaney EJ, Ullah AH (2005). Conservation of cysteine residues in fungal histidine acid phytases. Biochem. Biophys. Res. Commun. 328:404-408.
Neuwald AF, Liu JS, Lawrence CE (1995). Gibbs motif sampling: detection of bacterial outer membrane protein repeats. Protein Sci. 4:1618-1632.
Oakley AJ (2010). The structure of Aspergillus niger phytase PhyA in complex with a phytate mimetic. Biochem. Biophys. Res. Commun. 397:745-749.
Olczak M, Morawiecka B, Watorek W (2003). Plant purple acid phosphatases - genes, structures and biological function. Acta Biochim. Pol. 50:1245-1256.
Puhl AA, Greiner R, Selinger LB (2008). A protein tyrosine phosphatase-like inositol polyphosphatase from Selenomonas ruminantium subsp. lactilytica has specificity for the 5-phosphate of myo-inositol hexakisphosphate. Int. J. Biochem. Cell Biol. 40:2053-2064.
Puhl AA, Gruninger RJ, Greiner R, Janzen TW, Mosimann SC, Selinger LB (2007). Kinetic and structural analysis of a bacterial protein tyrosine phosphatase-like myo-inositol polyphosphatase. Protein Sci. 16:1368-1378.
Raboy V, Dickinson DB, Below FE (1984). Variation in Seed Total Phosphorus, Phytic Acid, Zinc, Calcium, Magnesium, and Protein among Lines of *Glycine max* and *G. soja1*. Crop Sci. 24:431-434.
Rao DE, Rao KV, Reddy VD (2008). Cloning and expression of *Bacillus* phytase gene (phy) in *Escherichia coli* and recovery of active enzyme from the inclusion bodies. J. Appl. Microbiol. 105:1128-1137.
Rao DE, Rao KV, Reddy TP, Reddy VD (2009). Molecular characterization, physicochemical properties, known and potential applications of phytases: An overview. Crit. Rev. Biotechnol. 29:182-198.
Reddy NR, Sathe SK, Salunkhe DK (1982). Phytates in legumes and cereals. Adv. Food. Res. 28:1-92.
Reddy VA, Venu K, Rao DE, Rao KV, Reddy VD (2009). Chimeric gene construct coding for bi-functional enzyme endowed with endoglucanase and phytase activities. Arch. Microbiol. 191:171-175.
Schenk G, Guddat LW, Ge Y, Carrington LE, Hume DA, Hamilton S, de Jersey J (2000). Identification of mammalian-like purple acid phosphatases in a wide range of plants. Gene 250:117-125.
Schenk G, Ge Y, Carrington LE, Wynne CJ, Searle IR, Carroll BJ, Hamilton S, de Jersey J (1999). Binuclear metal centers in plant purple acid phosphatases: Fe-Mn in sweet potato and Fe-Zn in soybean. Arch. Biochem. Biophys. 370:183-189.
Scott JJ (1991). Alkaline Phytase Activity in Nonionic Detergent Extracts of Legume Seeds. Plant Physiol. 95:1298-1301.
Selle PH, Ravindran V, Caldwell A, Bryden WL (2000). Phytate and phytase: consequences for protein utilisation. Nutr. Res. Rev. 13:255-

278.
Shin S, Ha NC, Oh BC, Oh TK, Oh BH (2001). Enzyme mechanism and catalytic property of beta propeller phytase. Structure 9:851-858.
Shivange AV, Schwaneberg U, Roccatano D (2010). Conformational dynamics of active site loop in *Escherichia coli* phytase. Biopolymers 93:994-1002.
Strater N, Klabunde T, Tucker P, Witzel H, Krebs B (1995). Crystal structure of a purple acid phosphatase containing a dinuclear Fe(III)-Zn(II) active site. Science 268:1489-1492.
Tamura K, Dudley J, Nei M, Kumar S (2007). MEGA4: Molecular Evolutionary Genetics Analysis (MEGA) software version 4.0. Mol. Biol. Evol. 24:1596-1599.
Thompson JD, Higgins DG, Gibson TJ (1994). CLUSTAL W: improving the sensitivity of progressive multiple sequence alignment through sequence weighting, position-specific gap penalties and weight matrix choice. Nucleic Acids. Res. 22:4673-4680.
Tye AJ, Siu FK, Leung TY, Lim BL (2002). Molecular cloning and the biochemical characterization of two novel phytases from *B. subtilis* 168 and *B. licheniformis*. Appl. Microbiol. Biotechnol. 59:190-197.
Ullah AH, Dischinger HC, Jr. (1993). *Aspergillus ficuum* phytase: complete primary structure elucidation by chemical sequencing. Biochem. Biophys. Res. Commun. 192:747-753.
Vohra A, Satyanarayana T (2003). Phytases: microbial sources, production, purification, and potential biotechnological applications. Crit. Rev. Biotechnol. 23:29-60.
Wodzinski RJ, Ullah AH (1996). Phytase. Adv. Appl. Microbiol. 42:263-302.
Wyss M, Brugger R, Kronenberger A, Remy R, Fimbel R, Oesterhelt G, Lehmann M, van Loon AP (1999). Biochemical characterization of fungal phytases (myo-inositol hexakisphosphate phosphohydrolases): catalytic properties. Appl. Environ. Microbiol. 65:367-373.
Xiang T, Liu Q, Deacon AM, Koshy M, Kriksunov IA, Lei XG, Hao Q, Thiel DJ (2004). Crystal structure of a heat-resilient phytase from *Aspergillus fumigatus*, carrying a phosphorylated histidine. J. Mol. Biol. 339:437-445.
Yang M, Johnson SC, Murthy PP (2012). Enhancement of alkaline phytase production in Pichia pastoris: Influence of gene dosage, sequence optimization and expression temperature. Protein Exp. Purif. 84:247-254.
Yang WJ, Matsuda Y, Sano S, Masutani H, Nakagawa H (1991). Purification and characterization of phytase from rat intestinal mucosa. Biochim. Biophys. Acta. 1075:75-82.
Zhang GQ, Dong XF, Wang ZH, Zhang Q, Wang HX, Tong JM (2010a). Purification, characterization, and cloning of a novel phytase with low pH optimum and strong proteolysis resistance from *Aspergillus ficuum* NTG-23. Bioresour. Technol. 101:4125-4131.
Zhang R, Yang P, Huang H, Shi P, Yuan T, Yao B (2011a). Two types of phytases (histidine acid phytase and beta-propeller phytase) in Serratia sp. TN49 from the gut of *Batocera horsfieldi* (coleoptera) larvae. Curr. Microbiol. 63:408-415.
Zhang R, Yang P, Huang H, Yuan T, Shi P, Meng K, Yao B (2011b). Molecular and biochemical characterization of a new alkaline beta-propeller phytase from the insect symbiotic bacterium *Janthinobacterium* sp. TN115. Appl. Microbiol. Biotechnol. 92:317-325.
Zhang Y, Liu C, Li Y, Wu K (2010b). Phytase transgenic maize does not affect the development and nutrition utilization of *Ostrinia furnacalis* and *Helicoverpa armigera*. Environ. Entomol. 39:1051-1057.
Zhao W, Xiong A, Fu X, Gao F, Tian Y, Peng R (2010). High Level Expression of an Acid-Stable Phytase from *Citrobacter freundii* in *Pichia pastoris*. Appl. Biochem. Biotechnol. 162:2157-65.
Zhu W, Qiao D, Huang M, Yang G, Xu H, Cao Y (2010). Modifying Thermostability of *appA* from *Escherichia coli*. Curr. Microbiol. 64:267-273.